Experimental observations of non-equilibrium distributions and transitions in a 2D granular gas

Jeffrey S. Urbach and Jeffrey S. Olafsen

Department of Physics, Georgetown University, Washington, DC 20057

Abstract. A large number (∼10,000) of uniform stainless steel balls comprising less than one layer coverage on a vertically shaken plate provides a rich system for the study of excited granular media. Viewed from above, the horizontal motion in the layer shows interesting collective behavior as a result of inelastic particle-particle collisions. Clusters appear as localized fluctuations from purely random density distributions, as demonstrated by increased particle correlations. The clusters grow as the medium is "cooled" by reducing the rate of energy input. Further reduction of the energy input leads to the nucleation of a collapse: a close-packed crystal of particles at rest. High speed photography allows for measurement of particle velocities between collisions. The velocity distributions deviate strongly from a Maxwell distribution at low accelerations, and show approximately exponential tails, possibly due to an observed cross-correlation between density and velocity fluctuations. When the layer is confined with a lid, the velocity distributions at higher accelerations are non-Maxwellian and independent of the granular temperature.

1 Introduction

The development of a kinetic theory of granular gases, collections of large numbers of inelastically colliding particles, has proven to be a very challenging undertaking. While the equilibrium properties of elastically colliding gases are relatively well understood, the introduction of physically relevant levels of dissipation change the dynamics dramatically. Considerable progress has been made in understanding the behavior of freely cooling granular gases, where the energy lost to collisions is not replaced. In order to model a variety of industrial processes where energy is added to the grains to enhance mixing and transport, a kinetic theory of forced granular gases is required. By analogy with the theory of equilibrium fluids, the goal is to solve a Boltzmann-like equation for the relevant 'microscopic' statistical distribution functions describing the behavior of individual grains. The rate at which energy is put into the fluctuating velocities is balanced by the rate at which it is lost in collisions. 'Macroscopic' transport coefficients, relating average fluxes (or currents) to gradients in local (coarse grained) variables, can then be calculated from the appropriate correlation functions.

Some progress has been made in building a continuum description of granular fluids from a microscopic kinetic theory, but has typically involved

a number of approximations that have yet to be tested. A hydrodynamic description is only possible if the spatial and temporal fluctuations in the flow are sufficiently localized to permit coarse graining. This may be the case if the granular system is large enough and the energy in the flow is high enough, but making this statement quantitative is very much an ongoing effort. Precise experimental measurements of the steady state statistical properties in a variety of granular fluids are essential to developing and testing generally applicable descriptions. We have been investigating the fluidized state and the fluidization transition in a simple representation of a granular material: a single layer of identical spherical particles. Using identical particles simplifies analysis of the system and allows for comparison with experimental and theoretical results derived for atomic and molecular dynamics. The use of a single granular layer, in combination with high speed imaging technology, allows for a thorough description of the granular system, including particle velocity distributions, correlation functions, and transport properties. We have found a complex phase diagram that bears many similarities to equilibrium two-dimensional systems, but we have also directly measured particle velocity distributions that are non-Maxwellian, and density correlation functions that show non-equilibrium effects [1]. We have also measured the cross-correlation between density and temperature fluctuations, and the effects of constraining the granular layer by placing a lid above it [2].

This paper is organized as follows: Section 2 describes the experimental setup and analysis techniques, and Section 3 describes the experimentally observed phase diagram. Our results on the statistical characterization of the granular gas are reported in 4, followed by a comparison with related work and a discussion of future directions in Section 5.

2 Experimental setup and methods

The experimental apparatus consists of a 20 cm diameter smooth, rigid aluminum plate that is mounted horizontally on an electromagnetic shaker that oscillates the plate vertically. The plate is carefully leveled, and the amplitude of acceleration is uniform across the plate to better that 0.5 %. The acceleration of the plate is monitored with a fast-response accelerometer mounted on the bottom surface of the plate. Two types of particles were used for the experiments described below: smaller spheres of 302 stainless steel with an average diameter of 1.191 $\pm$ 0.0024 mm, and larger spheres of 316 stainless with an average diameter of 1.588 $\pm$ 0.0032 mm. The coefficient of restitution, both particle-particle and particle-plate, is about 0.9. The particles are contained by an aluminum rim that occupies the outer 1.9 cm of the plate. The particles are illuminated by low angle diffuse light. This illumination produces a small bright spot at the top of each particle when viewed through a video camera mounted directly above the plate.

Two digital video cameras are used for data acquisition, a high-resolution camera for studying spatial correlations (Pulnix-1040, 1024 x 1024 pixels, Pulnix America, Inc., Sunnyvale, CA), and a high-speed camera for measuring velocity distributions (Dalsa CAD1, 128 x 128 pixels, 838 frames/second, Dalsa Inc., Waterloo, ON; Canada). A collection of images and movies is available for viewing at www.physics.georgetown.edu/∼granular. The acquired digital images are analyzed to determine particle locations by calculating intensity weighted centers of bright spots identified in the images.

The frame rate of the high speed camera is much faster than the inter-particle collision rate, so it is possible to measure particle velocities by measuring the displacement of the particle from one image to the next. The trajectories determined from the images are nearly straight lines between collisions. Although the frame rate is fast compared the collision time, the fact that it is finite introduces unavoidable systematic errors into the experimentally determined velocity distributions. Some particles will undergo a collision between frames, and the resulting displacement will not represent the true velocity of the particle either before or after the collision. Since fast particles are more likely to undergo a collision, the high energy tails of the distribution will be decreased. The probability that a particle of velocity v will not undergo a collision during a time interval Δt is proportional to $\exp(-v\Delta t/l_o)$, where l_o is the mean free path. The effect of this on the velocity distribution function reported here is quite small. In addition to taking velocities out of the tails of the distribution, collisions will incorrectly add the velocities of those particles elsewhere in the distribution. This effect can be minimized by filtering out the portion of particle trajectories where collisions occur. This is done by analyzing particle position in 3 images at a time. When the change in apparent velocity from the first two images differs from the change in the second two by more than a specified cutoff value, the points are neglected. Because a relatively small fraction of the particles undergo a collision between any two frames, the results are not sensitive to the precise value chosen. At the highest accelerations considered in this work, varying the cutoff value over more than an order of magnitude changes the measured granular temperature (*rms* velocity) by less than 10%, and the flatness of the distribution (Eq. 2) by less than 0.2. Similar issues are considered in a somewhat different manner in reference [3].

3 Phase diagram

When the plate oscillation amplitude is not too large, the spheres never hop over one another; thus the system essentially two-dimensional. Nonetheless, there is sufficient energy in the horizontal velocity component to generate fascinating dynamic phenomena. At moderately large sinusoidal vibration amplitudes, a fully fluidized state is observed. The spheres are constantly in motion and there is no large-scale spatial ordering. Figure 1(a) shows

an instantaneous image of part of a cell containing 8000 particles in this regime. (The number of particles in a single hexagonal close-packed layer is $N_{max} = 17275$ for the smaller particles, giving a reduced density $\rho = N/N_{max} = 0.463$.) The peak plate acceleration relative to the acceleration due to gravity, $\Gamma = A\omega^2/g$, is just over one. This phase is characterized by an apparently random distribution of particle positions and velocities. A sense of the dynamics can be gained from an average of 15 frames taken over a period of 1 s (Fig. 1(b)), which shows the lack of any stable structure. As the amplitude of the acceleration is slowly decreased, the average kinetic energy of the particles decreases, and localized transient clusters of low velocity particles appear. An instantaneous image in this regime (Fig. 1(c)) does not look very different from the one taken at higher acceleration, but in the time-averaged image (Fig. 1(d)) bright peaks are clearly evident, corresponding to low-velocity particles that have remained relatively close to each other over the time interval. In this regime, the clusters typically survive for 1-20 seconds. In the low density regions outside of the clusters, there are particles with anomalously high velocities, and these appear to be responsible for the breakup of the clusters. There are no attractive interactions between these particles; the cluster formation is a uniquely non-equilibrium phenomenon, resulting from the dissipation during inter-particle collisions, and the particle-plate dynamics.

When the amplitude of the vibration is decreased somewhat below that of Fig. 1 (c,d), the typical cluster size increases to 12-15 particles. Within a few minutes at this acceleration, one of these large clusters will become a nucleation point for a 'solid' phase, similar to what is referred to as 'inelastic collapse' [4]. The particles in the collapse are in contact with all of their neighbors, and form a perfect hexagonal lattice (Fig. 1(d)). The collapse is surrounded by a gas of the remaining particles. The sharp interface between the coexisting phases can be seen in the time-averaged image (lower panel of Fig. 1(e)) . The two-phase co-existence persists essentially unchanged for as long as the driving is maintained. At higher densities, instead of a transition directly from the clustering behavior to collapse, there is an intermediate phase with apparent long range order. Figure 1(g) shows a monolayer in this ordered state, where the spheres are arranged in a hexagonal lattice but are not at rest or in contact with one another. The disorder in the image is a consequence of the fluctuations induced by inter-particle collisions. When the particle positions in the ordered phase are averaged over a short time (Fig. 1(h)), the resulting image displays a nearly perfect lattice, with one unoccupied site. Measurements of the correlation functions for positional and orientational order parameters in this phase suggest that the transition to this ordered phase is quantitatively similar to the liquid-solid transitions observed in a variety of equilibrium systems.

Figure 2 shows phase diagrams of the system with two different densities. The data for the nucleation points were taken by decreasing the plate

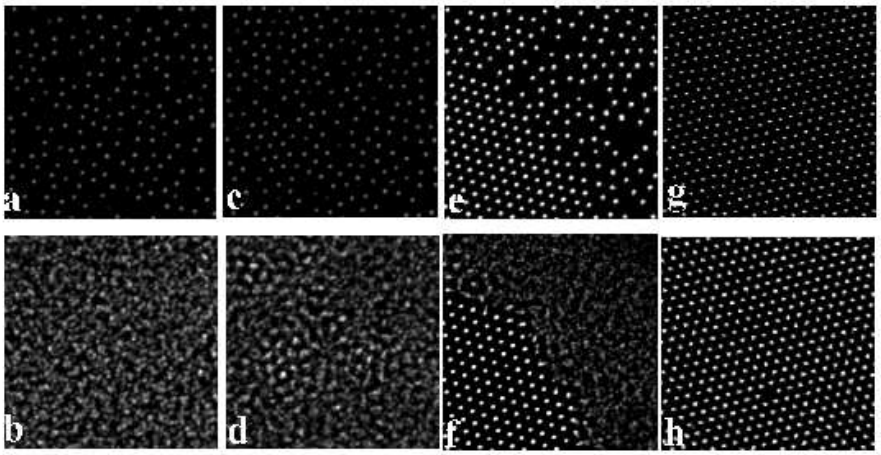

Fig. 1. Instantaneous (top row) and time-averaged (bottom row) photographs detailing the different phases of the granular monolayer. (a), (b), uniform particle distributions typical of the gas phase ($\rho = 0.463, \Gamma = 1.01, \nu = 70$ Hz). (c) The clustered phase ($\rho = 0.463, \Gamma = 0.8, \nu = 70$ Hz). The higher intensity points in a time-averaged image, (d), denote slower, densely packed particles. (e) A portion of a collapse for $\rho = 0.463$, $\Gamma = 0.76$, and $\nu = 70$ Hz. (f) The time-averaged image shows that the particles in the collapse are stationary while the surrounding gas particles continue to move. (g),(h) In a more dense system, $\rho = 0.839$, there is an ordered phase ($\Gamma = 1.0, \nu = 90$ Hz) where all of the particles remain in motion.

acceleration in steps of about $0.003g$, and waiting 5 minutes at each step to see if the collapse nucleates. The precise location of the nucleation line depends on the waiting time, but only very weakly. Once the collapse forms, increasing the acceleration causes it to 'evaporate' as particles return to the gas phase. Th open circles in Figure 2(a) indicate the acceleration required to fully evaporate the collapse. The evaporation line is omitted from the lower panel for clarity.

It is not immediately clear what causes the frequency dependence in the phase diagram. For an ideal spherical particle on an oscillating plate with a velocity-independent coefficient of restitution, the dynamical behavior depends only on Γ, and the frequency sets the timescale for the motion, and the length scale through g/ω^2, which is proportional to the distance a ball falls during one oscillation period. Thus as the frequency is reduced for fixed Γ, balls will bounce higher. Because the balls in this system interact with their neighbors, it is possible that the frequency dependence enters through the ratio of this length scale to the ball diameter. In fact, the rapid increase in the acceleration where collapse forms for frequencies below about 50 Hz (see Fig. 2) occurs when the particles begin to bounce high enough to hop over one another, resulting in a gradual transition from primarily 2D to 3D dynamics. This suggests that the frequency dependence comes from a char-

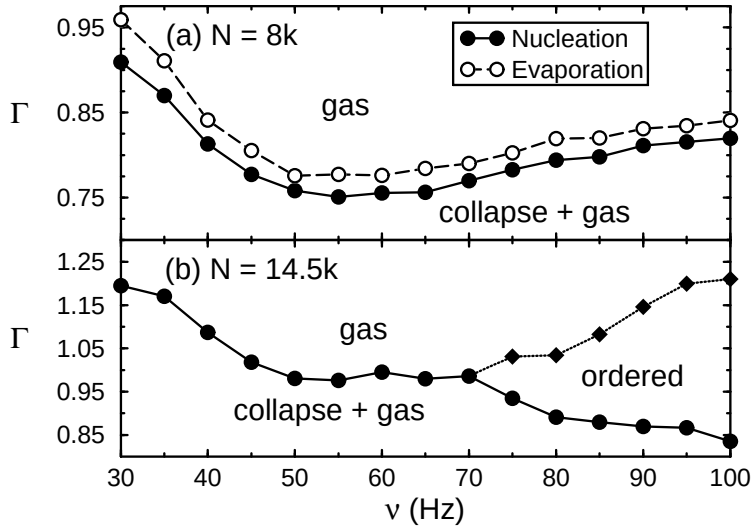

Fig. 2. The phase diagrams for (a) N = 8000 particles ($\rho = 0.463$) and (b) N = 14,500 ($\rho = 0.839$) particles. The filled circles denote the acceleration where the collapse nucleates. The open circles in (a) indicate the point where the collapse disappears upon increasing the acceleration. The diamonds in (b) show the transition to the ordered state as the acceleration is reduced.

acteristic frequency $\nu_c = (g/d)^{1/2}$, where d is the sphere diameter. Figure 3 shows the phase diagram measured for two different sets of particles determined at the same reduced density ρ, one with a diameter of 1.2 mm, and one with a diameter of 1.6 mm. The upturn at low frequencies and the appearance of the ordered phase occur at lower frequencies for the larger particles, but the scaled phase diagrams lie right on top of one another.

4 Statistical characterization of the granular gas

In order to incorporate the non-equilibrium fluctuations observed in Fig. 1(c,d) into a kinetic theory of the granular fluids, quantitative measures are required. In the monolayer system, particle positions can be directly determined from images acquired with a digital video camera. These can be used to evaluate statistical measures, such as the pair correlation function and the velocity distribution function, that are essential components of kinetic theory.

4.1 Pair Correlation Functions

Correlations in particle positions are most directly measured by the pair correlation function, $G(r)$:

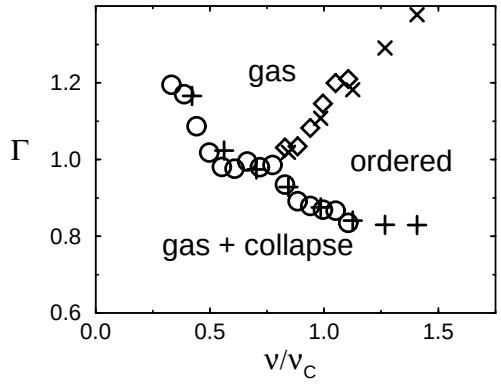

Fig. 3. The phase diagrams for 1.2 mm diameter particles (◯, ⋄) and 1.6 mm (+,×) at $\rho = 0.839$. The frequency is scaled by $\nu_c = (g/d)^{1/2}$.

$$G(r) = \frac{< \rho(0)\rho(r) >}{< \rho >^2}, \tag{1}$$

where ρ is the particle density. The correlations of a two-dimensional gas of elastic hard disks in equilibrium are due only to geometric factors of excluded volume and are independent of temperature [5].

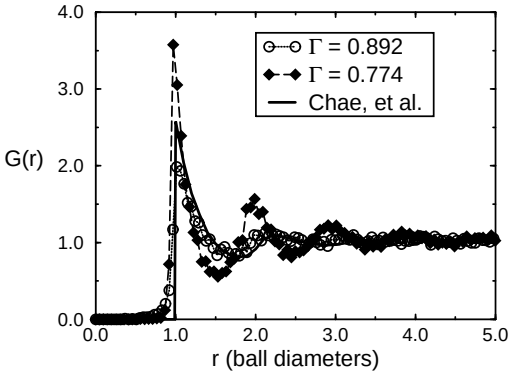

Fig. 4. The measured pair correlation function of a two-dimensional granular gas ($\rho = 0.463, \nu = 70$ Hz). The results are compared to the result from an equilibrium hard disk Monte Carlo calculation with no adjustable parameters. The legend gives the value of Γ.)

The solid line in Fig. 4 shows $G(r)$ from a Monte Carlo calculation of a two-dimensional gas of elastic hard disks in equilibrium for a density of 0.463

[6]. The experimentally measured correlation function in the gas-like phase, shown by the open circles, is almost identical to the equilibrium result. There are no free parameters in Fig. 4. The agreement between the experimental correlation function and the equilibrium result suggests that the structure in the correlation function of the gas-like phase is dominated by excluded volume effects. As the granular medium is cooled, the correlations grow significantly. This is evident from the data for a lower vibration amplitude ($\Gamma = 0.774$, just above the acceleration where the collapse forms), shown as filled diamonds in Fig. 4. The increased correlations indicate that there are non-uniform density distributions in the medium: high density regions of relatively closely packed particles, which must coexist with relatively low density regions. In the kinetic theory of equilibrium fluids, the pair correlation function plays a central role, because thermodynamic quantities can be written as integrals with $G(r)$. The equation of state for an equilibrium hard disk system, as well as the Enskog modification to the Boltzmann equation (the correction to account for excluded volume effects), depends on $G(r)$ at contact (r =1 diameter) [7]. Extensions of kinetic theory to inelastic gases [8] assume that $G(r)$ at contact is given by the Carnahan-Starling relationship [9], which works well for elastic gases. Thus the dramatic increase in correlations will likely have significant quantitative implications for transport coefficients in the granular gas.

At higher plate accelerations, the pair correlation function loses all of its structure. Fig. 5 shows $G(r)$ at $\Gamma = 0.93$, $\Gamma = 1.50$, and $\Gamma = 3.0$. Increasing the steady state kinetic energy of the granular gas by increasing the amplitude of the acceleration at constant frequency causes the gas to change from primarily two-dimensional, where the particles never hop over one another, to essentially three-dimensional. This transition can be observed in the pair correlation function, $G(r)$, by the increase in its value for $r < 1$. (The correlation function includes only horizontal particle separations.) This transition can affect the dynamics in several ways: the effective density is decreased, so that excluded volume effects are less important; the inter-particle collisions can occur at angles closer to vertical, affecting transfer of energy and momentum from the vertical direction to the horizontal; and the change in the dimensionality itself can have important consequences.

In order to separate these effects from the direct consequences of increasing the kinetic energy of the gas, a Plexiglas lid was added to the system at a height of 2.54 mm, or 1.6 ball diameters for the larger particles. For this plate-to-lid separation, the larger particles cannot pass over top of one another, although enough room remains for collisions between particles at sufficiently different heights to transfer momentum from the vertical to the horizontal direction.

Figure 6 shows the pair correlation functions measured with the lid on, and demonstrates that the particle-particle correlations persist and become independent of Γ when the system is constrained in the vertical direction.

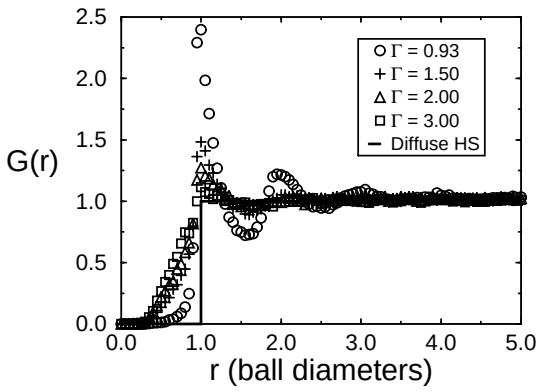

Fig. 5. (a) Pair correlation functions for larger accelerations in the unconstrained system. (◯) $\Gamma = 0.93$, (+) $\Gamma = 1.5$, (△) $\Gamma = 2.0$, (□) $\Gamma = 3.0$.

The correlation function decreases slightly from $\Gamma = 0.93$ to $\Gamma = 1.50$, and then remains essentially constant up to $\Gamma = 3$. The small value of $G(r)$ for distances less than one ball diameter indicates that the system remains 2D as Γ is increased. The structure observed in the correlation function is essentially the same as that of an equilibrium elastic hard sphere gas at the same density, indicating that the correlations that exist are due to excluded volume effects. From $\Gamma = 1.50$ to $\Gamma = 3.0$, the granular temperature changes by more than a factor of 2 (see Fig. 10), yet there is no detectable change in the pair correlation function. Thus, unlike the low acceleration behavior shown in Fig 4, the particle correlations in the constrained system at higher accelerations behave like those of a system of elastic hard disks.

4.2 Velocity Distribution Functions

A crucial ingredient of a statistical approach to describing the dynamics in a granular system is the velocity distribution, which may show non-equilibrium effects as can the correlation function. As described in section 2, the horizontal components of the particle velocities between collisions can be determined with the use of a high speed camera. Extensive measurement of the velocity distributions in the plane of the granular gas demonstrate non-Gaussian behavior.

The measured horizontal velocity distributions at $\Gamma = 0.93$, $\Gamma = 1.50$, and $\Gamma = 3.0$ are shown in Fig. 7. The distributions at low Γ are strongly non-Gaussian, showing approximately exponential tails [1]. As the acceleration is increased, the distribution crosses over smoothly to a Gaussian. This behavior is superficially similar to that of freely cooling granular media, where an initial Gaussian velocity distribution becomes non-Gaussian as the system cools, but these results are obtained in a steady state.

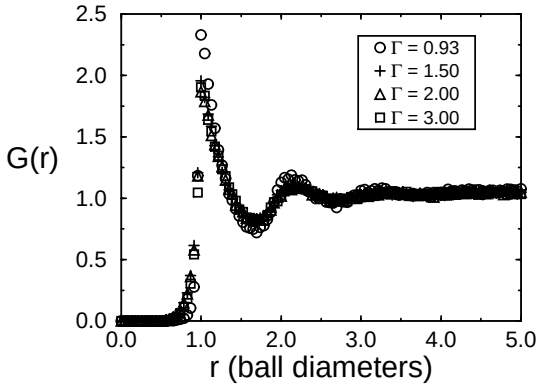

Fig. 6. Pair correlation functions for the velocity distributions where a lid constrains the system to remain two dimensional. The particle correlations remain as the shaking amplitude is increased. (◯) $\Gamma = 0.93$, (+) $\Gamma = 1.5$, (△) $\Gamma = 2.0$, (□) $\Gamma = 3.0$.

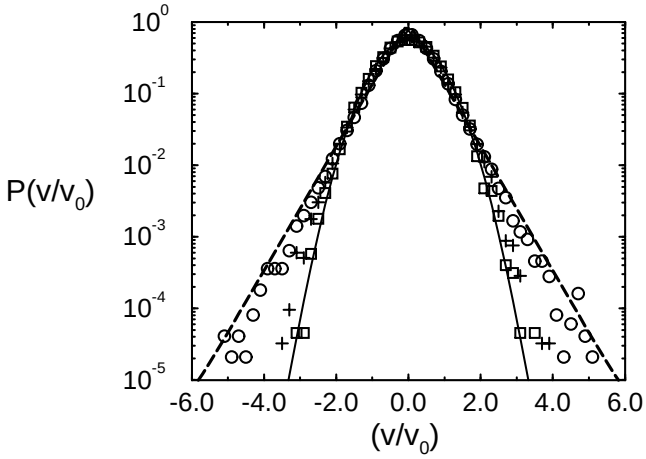

Fig. 7. Velocity distributions for the system without a lid. As the acceleration is increased, the distributions go from having nearly exponential tails to Gaussian tails. (◯) $\Gamma = 0.93$, (+) $\Gamma = 1.5$, (□) $\Gamma = 3.0$.

The non-Gaussian velocity distributions observed at low accelerations are accompanied by clustering, as demonstrated by a dramatic increase in the structure of the pair correlation function. Conversely, the crossover to Gaussian velocity distributions is accompanied by the disappearance of spatial correlations, consistent with the suggestions that the non-Gaussian velocity distributions arise from a coupling between density and temperature fluctuations [10].

The velocity distributions measured with the lid on are shown in Figure 8. The crossover to Gaussian distributions observed when the acceleration is increased in the unconstrained system is not observed. Instead, like the pair correlation function, the statistical characteristics of the granular gas become independent of acceleration, and therefore independent of the granular temperature. The tails of the distribution in the constrained system are consistent with $P(v) \propto \exp(-|v|^{3/2})$, as observed in [3] and predicted by [11]. The relationship between our results and that work is discussed in section 5.2.

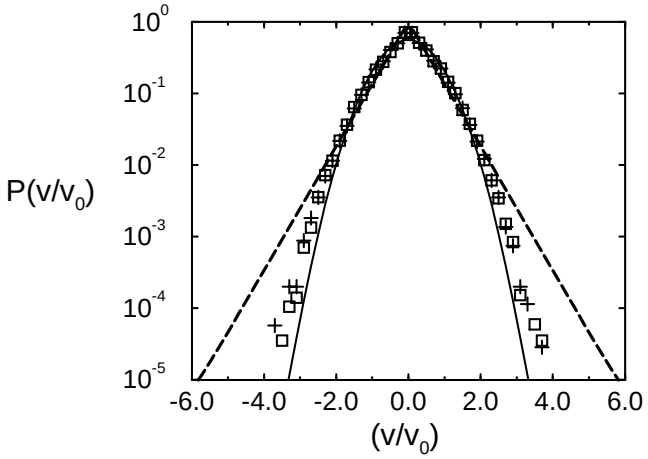

Fig. 8. Velocity distributions for the system with a lid. The scaled distributions are essentially independent of acceleration. (+) $\Gamma = 2.0$, (□) $\Gamma = 3.0$.

In order to more clearly display the evolution of the distributions, we use a simple quantitative measure of the normalized width of the distribution, the flatness (or kurtosis):

$$F = \frac{< v^4 >}{< v^2 >^2}. \tag{2}$$

For a Gaussian distribution, the flatness is 3 and for the broader exponential distribution, the flatness is 6. In the absence of a lid, the flatness demonstrates a smooth transition from non-Gaussian to Gaussian behavior as the acceleration is increased (Fig. 9), whether the smaller (circles) or larger (stars) particles are used. With the lid on, the velocity distributions remain more non-Gaussian than in the free system for identical accelerations (or identical granular temperatures) and density (diamonds).

The crossover from Gaussian to non-Gaussian behavior observed without the lid is therefore not simply an effect of increasing the vertical kinetic energy

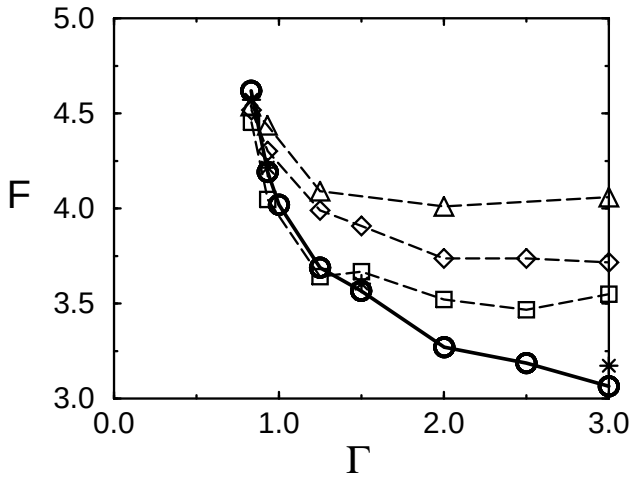

Fig. 9. Plot of the flatness as a function of granular temperature with and without a lid in the system. At low Γ the system is nearly 2D and the lid has no effect. Data for $\rho = 0.532$: (◯) d = 1.2 mm and (∗) d = 1.6 mm without lid; (◇) d = 1.6 mm with lid. Data for $\rho = 0.478$ (△) and $\rho = 0.611$ (□) with a lid and d = 1.6 mm.

of the particles, but rather related to the transfer of energy from the vertical to horizontal motion in the system via collisions, the change in the density, or the change in dimensionality of the gas.

To determine the relative contribution of density changes to the non-Gaussian velocity distributions in the gas, the number of particles on the plate was increased by 15% and decreased by 10% from the value of $\rho = 0.532$ and the lid was kept on. For all accelerations, the flatness decreased with increased density. This surprising result may be related to the fact that strongly non-Gaussian distributions observed at low Γ are accompanied by strong clustering [1]. If the average density is increased, the larger excluded volume means that less phase space remains for fluctuations to persist. The fact that increasing the density with the lid on makes the velocity distribution more Gaussian suggests that the crossover to Gaussian observed without the lid is not due to the decrease in density of the gas.

In addition to providing velocity distribution functions, measurements of the particle velocities can be used to calculate the granular temperature, $T_G = (1/2) < v^2 >$. Figure 10 shows the granular temperature versus plate acceleration for several different experimental configurations. At low acceleration ($\Gamma \leq 1$), very few particles strike the lid and the lid has no significant effect. At larger Γ it is clear that the horizontal granular temperature is reduced when a significant number of particles strike the lid. It is interesting to note that T_G approaches zero linearly at finite Γ, indicating that the re-

lationship between the driving and the horizontal granular temperature is of the form $T_G \propto \Gamma - \Gamma_c$. Existing models for the scaling of T_G with Γ predict a relationship of the form $T_G \propto \Gamma^{\theta}$ [12,13,14]. Those results are only valid at relatively large accelerations, and clearly do not correctly describe the behavior shown in Fig. 10.

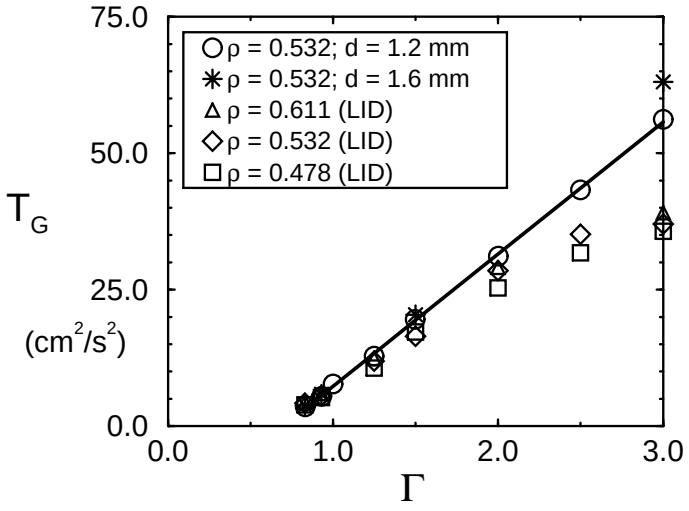

Fig. 10. Plot of the horizontal granular temperature, T_G, as a function of dimensionless acceleration, Γ, with and without a lid. Without the lid (◯,∗) the system becomes three dimensional at high accelerations.

4.3 Density-Velocity cross-correlations

Some insight into the origins of the non-Gaussian velocity distributions can be obtained by investigating the relationship between the local *fluctuations* in density and kinetic energy. Puglisi *et al.* [10] have proposed a model which relates strong clustering to non-Gaussian velocity distributions in a driven granular medium. In their framework, at each local density the velocity distributions are Gaussian, and the non-Gaussian behavior arises from the relative weighting of the temperature by local density in the following manner:

$$P(v) = \sum_N n(N) e^{-\left(\frac{v^2}{v_0^2(N)}\right)} \tag{3}$$

where N is the number of particles in a box, $v_0^2(N)$ is the second moment of the distribution of velocities for boxes with N particles, and $n(N)$ is the number of boxes that contain N particles. In this model, the local temperature

is a decreasing function of the local density, and the velocity distributions conditioned on the local density are Gaussian.

We have investigated the velocity distributions conditioned on the local density by examining the distribution of velocities for data at a constant number of particles in the frame of the camera. In the strongly clustering regime, we do observe a direct correlation between local density and temperature. Figure 11 is a plot of the local temperature as a function of particle number in the camera frame normalized by the global granular temperature.

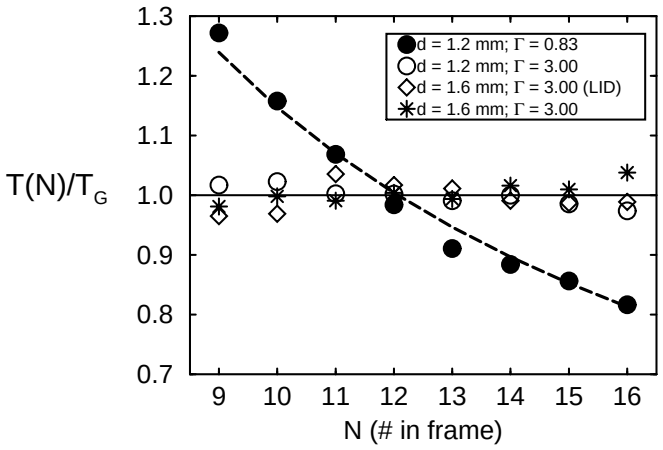

Fig. 11. Plot of $T(N)/T_G$ where N is the number of particles in the camera frame (see text). At low Γ, the local temperature and density are strongly correlated. At high Γ, the local granular temperature is independent of density, even when the velocity distributions remain non-Gaussian in the constrained system. $\rho = 0.532$. The area of the camera frame was approximately 24 ball areas.

The result at low accelerations is similar to the model of Puglisi *et al.* [10]: When the particle-particle correlations are strongest (and larger than those of an equilibrium hard sphere gas [1]), there is a density dependence to the granular temperature (filled circles). At $\Gamma = 3$, where all of the particles are essentially uncorrelated in a 3D volume in the absence of a lid, there is no density dependence (open circles, stars). However, even in the confined system at $\Gamma = 3$, where the distribution is still not Gaussian, no appreciable density dependence is observed (diamonds), suggesting that the non-Gaussian velocity distributions and density-dependent temperature are not as simply related as they are in the model of Puglisi *et al.* [10]. In fact, while there is a clear density dependence on the local temperature at low Γ, the measured velocity distribution conditioned on the local density is not Gaussian. At each density, the conditioned velocity distribution function is almost identical to that of the whole: when the entire distribution is non-

Gaussian, the distribution at a single density is non-Gaussian, and when the whole is Gaussian, each conditional velocity distribution is Gaussian.

A more general form of Eq. 3 represents the total velocity distribution as a product of local Gaussian velocity distributions with a distribution of local temperatures:

$$P(v) = \int f(T(\boldsymbol{r},t))e^{-(\frac{v^2}{2T(\boldsymbol{r}(t))})}d\boldsymbol{r}dt \tag{4}$$

where $T(\boldsymbol{r},t)$ is the local temperature that is varying in space and time. Conditioning on the local temperature would then recover the Maxwell statistics underlying the fluctuations.

Performing this analysis on our data does not succeed in producing Maxwell statistics. Within small windows of local temperature, the distributions remain non-Gaussian. Indeed, the analysis can be extended to condition on both the local temperature and density in the system, but with similarly limited success except for the lowest local temperatures, although all of the conditioned distributions are closer to Gaussian than the full distribution. A plot of the flatness of the conditioned distributions measured at $\Gamma = 0.83$ is shown in Fig. 12. For each density (number of particles in the frame of the camera) the flatness is close to 3 for the 'coolest' fluctuations, but systematically increases for larger local temperatures. The flatness of the full distribution for the data shown in the figure is 4.7.

If all of the measured velocities are normalized by the local granular temperature and combined into a single distribution, that distribution is Gaussian, as observed in a simulation of vibrated granular media [15]. This is a rather surprising result, and the origin of this behavior is not understood.

5 Discussion

5.1 Clustering and Collapse

An understanding of the interesting dynamics displayed in both the gas phase and the two-phase coexistence regions will require a better understanding of the flow of energy from the plate to the granular layer. Energy flow into thicker layers from a vibrating surface have been extensively studied, but the dynamics of the monolayer system are quite different [12,13,14]. Energy is dissipated much more slowly than in thicker layers, and therefore the chaotic dynamics of particles on an oscillating plate must be considered [16,17]. The net energy transferred to the vertical motion by the plate must balance the energy dissipated by inter-particle collisions. It is this balance that determines the steady-state horizontal granular temperature. In order to generate an equation of state, an expression for the energy input by the plate is required. The motion of a single ball on a plate displays the characteristics of low-dimensional chaos, but when coupled with a large number of similar systems

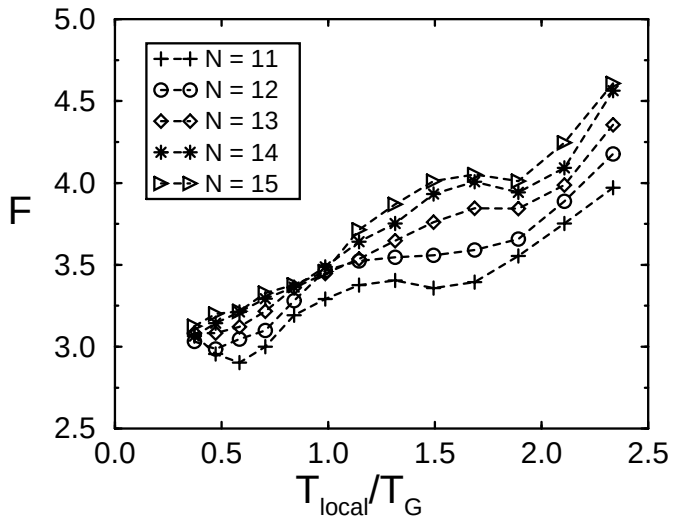

Fig. 12. Flatness of the velocity distribution conditioned on local granular temperature and local density. The velocity data is separated according to the number of particles in the frame of the camera (N), and the local granular temperature (T_{local}) determined from all of the particles in the frame. T_G is the granular temperature averaged over all of the frames. Data is for $\rho = 0.532$, $\Gamma = 0.83$, $\nu = 80$ Hz.

through inter-particle collisions, the result is apparently a very regular rate of energy flow, producing a system that looks in many ways very much like an equilibrium system of a large number of interacting particles [17].

The interaction of the spheres with the plate, in particular the apparent lack of any periodic or chaotic attractors with average energies less than the period-one orbit, may partially explain the two-phase coexistence and hysteresis observed in this system [16]. If the kinetic energy of the spheres drops too low, they will fall into the 'ground state', where they remain at rest on the plate, and the energy input drops to zero. Collisions from neighboring spheres may keep a sphere from falling into the ground state, but also dissipate energy. Quantitative predictions of the conditions under which density fluctuations can nucleate a collapse, as well as the stability of the collapse-gas interface, may be derivable from considerations of the sphere-plate dynamics, coupled with the kinetic theory of dense, inelastic gases.

The appearance of strong clustering and associated nearly exponential velocity distributions at low accelerations may also be strongly influenced by ball-plate dynamics. The clusters are low energy regions of the system, and at low plate accelerations the rate of energy input may be a strong function of average particle energies, thereby enhancing the clustering tendency of inelastic particles. The details of this process are specific to our system, but

all excited granular media require external forcing, and the rate of energy input is typically not independent of the dynamics of the grains themselves.

5.2 Two Dimensional Granular Gas

The granular layer at relatively high accelerations when constrained with a lid appears to be well suited for comparison with recent theoretical work on forced granular gases [11,19]. The unusual behavior of the system at low accelerations appears to be intimately tied to the interaction of the balls with the plate, and the unconstrained system at high accelerations has a somewhat ill-defined density. In contrast, once the average kinetic energy of the particles in the constrained system is large enough that the particles can explore the entire volume of the cell, the effective density does not vary with acceleration. Our results show that the correlations and velocity distributions that are independent of Γ, and so do not appear to be very sensitive to the details of the energy input. (Although the way energy is transferred from the vertical direction to the horizontal, through collisions between particles at heights that are not too different, may have important implications.)

As described in section 4.2, the tails of the velocity distribution in this regime are reasonably well described by $P(v) \propto \exp(-|v|^{3/2})$, in agreement with recent experimental and theoretical results. However, the details of how energy is transferred to the horizontal motion in the shaking experiments are sufficiently complicated that the agreement with the theoretical calculation of van Noije, et al.,[11] is perhaps surprising. Furthermore, the experimental system of Losert, et al.,[3] was not constrained to be two-dimensional, but they do not obtain the crossover to Gaussian measured in our system without the lid.

In the calculations of van Noije, et al., the inelastic particles are forced by uncorrelated white noise. In the experiment, the energy is input into the horizontal velocities from the vertical velocity via collisions. Given the complex dynamics of the system, the collisional forcing may be reasonably well described by uncorrelated accelerations, but the forcing occurs only during inter-particle collisions. For accelerations that occur much less frequently than the inter-particle collision times, the velocity distribution should approach the freely cooling result ($P(v) \propto \exp(-|v|)$) [18], whereas white noise forcing is well modeled by accelerations that occur on timescales much faster than the inter-particle collision time [10]. However, a recent numerical simulation of white noise forcing [19] found empirically that the behavior of the system was independent of the ratio between the rate of accelerations and the rate of collisions as long as the ratio was greater than one. This result suggests that the van Noije, et al., calculations are in fact valid for the granular monolayer, and the agreement between theory and experiment is not simply fortuitous.

Both our experiments and the results of Losert, et al., are consistent with velocity distributions that behave like $P(v) \propto \exp(-|v|^{3/2})$ in the tails, but we obtain that result only when the system is tightly constrained so that particles

cannot pass over one another, whereas the lid of the cell used by Losert et al., is 5 ball diameters above the plate. Furthermore, Losert et al., include measurements up to $\Gamma = 8$, whereas the our results for an unconstrained layer show a velocity distribution that becomes almost completely Gaussian when Γ is increased to 3. There are several differences between the systems (stainless steel spheres on an aluminum plate vs. glass beads on Delrin in Losert, et al.), that might effect the results, but the most significant difference may be that suggested by Figure 3, that the dynamics of the layer for a particular coverage are governed by Γ and the ratio of the driving frequency to $\nu_c = (g/d)^{1/2}$, where d is the sphere diameter. Since even our largest particles are 2.5 times smaller than the glass beads used by Losert, et al., our measurements at $\nu = 70$Hz are in a different regime than their measurements at $\nu = 100$Hz. In particular, our system at $\Gamma = 3$ may be more fully three dimensional than that of Losert, et al., and $\Gamma = 8$. Consistent with this picture, Losert, et al. do find that the $\exp(-|v|^{3/2})$ scaling fails for lower frequencies. However, their measured velocity distribution does not appear closer to Gaussian, as might be expected from our results.

In summary, the vibrated granular monolayer has proved to be a rich testbed for the non-equilibrium dynamics of excited granular media. The ability to precisely measure statistical distribution functions under well controlled experimental conditions should allow for careful tests of the predictions of kinetic theory. A complete understanding of the dynamics will require a thorough study of the phase space, as well as a more careful consideration of the dynamics of energy transfers in the system.

6 Acknowledgments

This work was supported by an award from the Research Corporation, a grant from the Petroleum Research Fund and grant DMR-9875529 from the NSF. One of us (JSU) was supported by a fellowship from the Sloan Foundation.

References

*. e-mail: urbach@physics.georgetown.edu

1. J. S. Olafsen and J. S. Urbach, Phys. Rev. Lett. **81**, 4369 (1998).
2. J. S. Olafsen and J. S. Urbach, to appear in Phys. Rev. E.
3. W. Losert, D. G. W. Cooper, J. Delour, A. Kudrolli, and J. P. Gollub, to appear in Chaos.
4. S. McNamara and W. R. Young, Phys. Rev. E **53**, 5089 (1996).
5. L. D. Landau and E. M. Lifshitz, *Statistical Physics* (Pergamon Press, Oxford, 1980).
6. D. G. Chae, F. H. Ree, and T. Ree, J. Chem. Phys. **50**, 1581 (1969); interpolated for $\rho = 0.463$.
7. J. P. Hansen and I. R. McDonald, *Theory of Simple Liquids*, 2nd ed. (Academic Press, New York, 1986).

8. J. T. Jenkins and M. W. Richman, Phys. Fluids **28**, 3485 (1985).
9. N. F. Charnahan and K. E. Starling, J. Chem. Phys. **51**, 635 (1969).
10. A. Puglisi, V. Loreto, U. M. B. Marconi, A. Petri, and A. Vulpiani, Phys. Rev. Lett. **81**, 3848; A. Puglisi, V. Loreto, U. M. B. Marconi, and A. Vulpiani, Phys. Rev. E. **59**, 5582. (1998).
11. T. P. C. van Noije and M. H. Ernst, Granular Matter **1**, 57 (1998).
12. S. McNamara and S. Luding, Phys. Rev. E **58**, 813 (1998).
13. J. M Huntley, Phys. Rev. E **58**, 5168 (1998).
14. E. Falcon, S. Fauve, C. Laroche, European Physical Journal B, **9**, 183 (1999).
15. C. Bizon, PhD. Thesis, University of Texas at Austin, 1998.
16. W. Losert, D. G. W. Cooper, and J. P. Gollub, Phys. Rev. E **59**, 5855 (1999).
17. J. S. Urbach and J. S. Olafsen, Proceedings of the 5th Experimental Chaos Conference, to appear.
18. S. E. Esipov and Th. Pöschel, J. Stat. Phys. **86**, 1385 (1997).
19. C. Bizon, M. D. Shattuck, J. B. Swift, and H. L. Swinney, Phys. Rev. E, to appear.